Physica E 60 (2014) 37–41

Contents lists available at ScienceDirect

Physica E

journal homepage: www.elsevier.com/locate/physe

Tunable passband in one-dimensional phononic crystal containing a piezoelectric $0.62Pb(Mg_{1/3}Nb_{2/3})O_3$–$0.38PbTiO_3$ single crystal defect layer

Yuling Wang [a,b], Wei Song [a], Enwei Sun [a], Rui Zhang [a,*], Wenwu Cao [a,c]

[a] Condensed Matter Science and Technology Institute, Harbin Institute of Technology, Harbin 150080, China
[b] Physical and Electrical Information Engineering Institute, Daqing Normal University, Daqing 163712, China
[c] Materials Research Institute, The Pennsylvania State University, University Park, PA 16802, USA

HIGHLIGHTS

- Investigation of band structure in 1D phononic crystal containing a PMN–0.38PT defect layer.
- Tunable frequency location of passband by external voltage on piezoelectric defect layer.
- Dependence of passband bandwidth on the acoustic impedance ratio of constitutive layer.

ARTICLE INFO

Article history:
Received 22 December 2013
Received in revised form
31 January 2014
Accepted 1 February 2014
Available online 8 February 2014

Keywords:
Phononic crystal
Tunable passband
Defect layer
PMN–0.38PT

ABSTRACT

Longitudinal acoustic wave propagation in one-dimensional phononic crystal containing a 0.2 mol% Fe-doped relaxor-based ferroelectric $0.62Pb(Mg_{1/3}Nb_{2/3})O_3$–$0.38PbTiO_3$ (PMN–0.38PT) single crystal defect layer is theoretically studied using the transfer matrix method. A passband can be produced in the stopband when the inserted PMN–0.38PT layer with thickness around its half wavelength. The frequency of the passband is closely dependent on the PMN–PT strain coefficient, suggesting that the band structure of phononic crystal is tunable by applying external electric field onto the piezoelectric crystal. Also, we investigated the influence of acoustic impedance of periodic constitutive materials (layers A and B) on the passband, where the bandwidth of the new passband becomes narrower as the acoustic impedance ratio of layer A and B (Z_A/Z_B) increase. The simulated results provide valuable guidance for designing tunable acoustic filters and switches made of phononic crystal consisting of the piezoelectric defect layer.

1. Introduction

Phononic crystals are made of periodic arrays of elastic inclusions in an elastic matrix. Due to the geometry and composition characteristics, it exhibits forbidden gaps of elastic/acoustic wave propagation in the band structure, regardless of wave polarization and propagation directions [1,2]. Typical band gap features can be used to design acoustic devices, such as acoustic/elastic filters, acoustic waveguides, noise control, and improvements in transducer design [3–7]. In addition, acoustic wave dispersion is observed in the band structure of phononic crystals, and thus they are potentially useful in the development of high-resolution acoustic focusing and the acoustic beam autocollimation [8,9]. Moreover, some authors proposed that the passband can be induced inside the stopband by introducing a defect into perfect periodic phononic crystal, which can be used as selective filters or demultiplexing of acoustic waves [10,11].

For some acoustic devices, it is useful to realize tunable phononic crystals, so as to control the band structures, including the existence, location and bandwidth of the stopband and/or passband [12,13]. In order to achieve tunable passband and stopband in phononic crystals, some functional materials were introduced into the periodic structure such as thermally activated shape memory alloy, electrorheological material, dielectric elastomer layer, and magnetoelastic

* Corresponding author. Tel.: +86 0451 86402797.
E-mail address: ruizhang_ccmst@hit.edu.cn (R. Zhang).

http://dx.doi.org/10.1016/j.physe.2014.02.001
1386-9477

material [14–17]. By changing the geometry of the inclusions or by varying the elastic characteristics of the constitutive materials through external stimuli, the band structure of phononic crystal can be adjusted.

Recently, interests in the band structures of phononic crystals based on piezoelectric materials have grown because of their high electromechanical coupling factor and low acoustic impedance [18,19]. More importantly, piezoelectric materials have some advantages over other types of tunable materials, such as shape memory alloys, electro-rheological materials, etc., in terms of accurate control of displacement, quick response time, and small device size [20]. Relaxor-based ferroelectric single crystal, such as $(1-x)Pb(Mg_{1/3}Nb_{2/3})O_3$–$xPbTiO_3$ (PMN–xPT), is very attractive for this application because it demonstrates much better piezoelectric and electromechanical coupling properties than the piezoelectric ceramic [21,22]. Due to the high anisotropy, phononic crystal containing the PMN–0.28PT single crystal poled along different directions shows significant difference in acoustic wave propagation characteristics [23]. The aged 0.2 mol% Fe-doped PMN–0.38PT single crystal is capable of generating a giant recoverable strain due to its reversible domain-switching mechanism [24]. A 0.8% strain can be reached in the $[0\,0\,1]_c$-oriented tetragonal crystal at 1.2 kV/mm external electric field. Moreover, the piezoelectric single crystal has very good temperature stability in a wide temperature range, demonstrating a large electrostrain from room temperature up to 160 °C.

In this paper, we propose theoretically a novel tunable phononic crystal with a defect mode by inserting an aged 0.2 mol% Fe-doped PMN–0.38PT layer into a one-dimensional (1D) phononic crystal. The transfer matrix method was employed to obtain the band structure and to study the passband. We investigated the dependence of passband on the thickness/strain of the piezoelectric defect layer whose thickness can be nonlinearly adjusted by the external electric field. Also, the effect of acoustic impedance of constituent materials (layers A and B) on the band structure was calculated. The simulated results provide theoretical foundation for the design of acoustical filters and acoustic switches.

2. Model and methods

The 1D phononic crystal structure is shown in Fig. 1. The system is composed of periodically alternating layers A and B with thickness d_A and d_B, respectively. Layer C is positioned in the middle of the periodic structure as a defect layer. Thus, the 1D phononic crystal has mirror symmetry about the layer C, and there are two A/B unit cells on each side.

Here, we used the transfer matrix method to study the acoustic wave propagation in 1D phononic crystal. For a normal incident

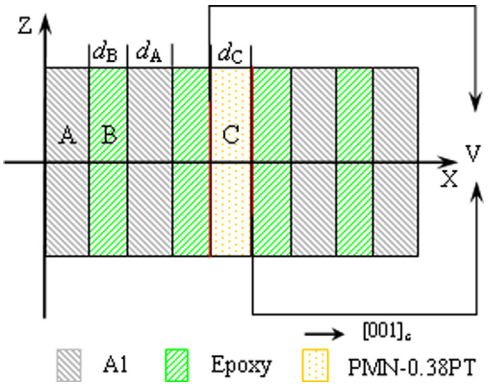

Fig. 1. Structure diagram of the one dimensional (1D) phononic crystal with a 0.2 mol% Fe-doped PMN–0.38PT defect layer.

longitudinal acoustic wave propagating through the phononic crystal from the left to the right, the pressure of the elastic wave in the medium is governed by the following wave equation,

$$\frac{1}{c_i^2}\frac{\partial^2 p}{\partial^2 t^2}-\nabla^2 p=0 \tag{1}$$

where c_i is the elastic wave phase velocity, and the subscript i represents the corresponding layer (A–C). The 1D plane wave solution of Eq. (1) is given by

$$p_i=P_i(x)e^{-i\omega t}=(A_i e^{ik_i x}+B_i e^{-ik_i x})e^{-i\omega t} \tag{2}$$

where the first and second terms on the right side of Eq. (2) represent the forward and reflected waves, respectively, $k_i=2\pi f/c_i$ is the wave number, and f is the wave frequency.

The continuity requirements for wave function and the normal stress at the interface between the sub-layers lead to the following relations [25],

$$M_{ij}=\frac{1}{2}\begin{bmatrix}\frac{Z_j+Z_i}{Z_j}&\frac{Z_j-Z_i}{Z_j}\\ \frac{Z_j-Z_i}{Z_j}&\frac{Z_j+Z_i}{Z_j}\end{bmatrix} \tag{3}$$

$$M_i=\begin{bmatrix}e^{-ik_i d}&0\\0&e^{-ik_i d}\end{bmatrix} \tag{4}$$

where M_{ij} is the wave matrix at the interface of sub-layers, M_i is the matrix of wave through the same layer, and $Z_i=\rho_i c_i$ is the acoustic impedance of the corresponding layer with the density ρ_i and thickness d_i.

According to the continuity conditions, the incident wave state vector P_0 and the transmitted wave state vector P_N has the following relationship,

$$\overrightarrow{P_0}=M\overrightarrow{P_N}=\begin{bmatrix}M_{11}M_{12}\\M_{21}M_{22}\end{bmatrix}\overrightarrow{P_N} \tag{5}$$

$$\overrightarrow{P}_0=(A_0e^{ik_0x},B_0e^{-ik_0x}) \tag{6}$$

$$\overrightarrow{P}_N=(A_Ne^{ik_0x},0) \tag{7}$$

where M is the relation matrix, and N is the number of cells. M can be expressed by

$$M=M_{01}M_1M_{12}M_2M_{21}\cdots M_{23}M_3M_{32}\cdots M_{12}M_2M_{21}M_1M_{10} \tag{8}$$

The transmission coefficient of 1D phononic crystal containing a piezoelectric layer can be represented by

$$T=|t|^2=\left|\frac{A_N}{A_0}\right|^2=\left|\frac{1}{M_{11}}\right|^2 \tag{9}$$

Based on Eqs. (3)–(9), the band structure of 1D phononic crystal can be simulated. In this work, we introduced an aged 0.2 mol% Fe-doped piezoelectric PMN–0.38PT single crystal as the defect layer C due to its giant recoverable field induced strain [24]. Its $[0\,0\,1]_c$ pseudo-cubic direction is parallel to the x-axis, and its thickness d_C can be adjusted by applying the external electric field [24]. In order to realize the expansion and compression of the single crystal, the compliant electrodes, such as carbon conductive grease, can be smeared onto the surface of the defect layer [16]. Because the applied compliant electrode is very thin, we can ignore its impact on wave propagation. The whole phononic crystal is merged into water, and the incident longitudinal acoustic wave has the center frequency f_0 at 1 MHz and frequency range investigated is from 0 to 2 MHz. We first investigated the band structure in the phononic crystal consisting of aluminum (Al, layer A) and epoxy (layer B) with their respective thickness to be $d_A=c_A/4f_0$ and $d_B=c_B/4f_0$. The defect layer C has an adjustable thickness of $d_C=xc_C/2f_0$, where the variable x is associated with the strain of

Table 1
Material properties used in the calculation.

Materials	ρ (kg/m^3)	c_l (m/s)	Z (MRayls)
Water	1,000	1480	1.48
Epoxy	1,180	2535	2.99
MgO	1,740	5790	10.07
Al	2,700	6400	17.28
Pb	11,400	2160	24.62
PZT-5H $[0\ 0\ 1]_c$[a]	7,360	4294	31.60
0.2 mol% Fe-doped PMN–0.38PT $[0\ 0\ 1]_c$[b]	8,093	4410	35.69
0.26PIN–0.42PMN–0.32PT $[0\ \bar{1}\ 1]_c$[c]	8,185	5119	41.90
Cu	8,950	5935	53.11
W	19,100	5680	108.50

[a] Taken from Ref. [30]
[b] Taken from Ref. [31]
[c] Taken from Ref. [32].

piezoelectric PMN–0.38PT single crystal that depends on the external electric field. Further, we studied the effects of the acoustic impedance of the constituent cells (e.g. layers A and B) on the passband, in which the material of layer A was changed but layers B and C remained unchanged. The parameters of all materials are given in Table 1.

3. Results and discussion

3.1. Effect of defect layer thickness on passband

Fig. 2 shows the transmission spectrum of the longitudinal acoustic wave through the phononic crystal along x-axis. The transmission coefficients of acoustic wave in the frequency range of 0–2 MHz are calculated using the transfer matrix method. Fig. 2(a) shows the transmission spectrum of the perfect phononic crystal composed of Al (layer A) and epoxy (layer B) without the defect layer. A typical propagation feature with an acoustic band gap from 0.39 MHz to 1.59 MHz can be observed. In Fig. 2(b), we studied the acoustic propagation in a phononic structure inserted by a PMN–0.38PT defect layer with the thickness of $c_C/4f_0$, which represents a slightly broadened forbidden band compared to the structure without the defect single crystal. In Fig. 2(c), the gap width of forbidden band was further enlarged in the phononic crystal containing the defect PMN–0.38PT layer with thickness of $c_C/2f_0$. Interestingly, a pass band appears at the center of the band gap (1 MHz), which is characterized by the transmission peak of 100% and the full width at half maximum (FWHM) of about 1.2 kHz.

Based on Fabry–Perot interferometric principle, a defect mode can be induced in the periodic structure when inserting a layer with the thickness of an integer multiple of its half wavelength, i.e. $2k_3d_3 = 2\pi n$, $n=1, 2, 3, \ldots$ [26]. Thus, the results in Fig. 2(b) and (c) show a good agreement with the theory. Here, we introduced the defect PMN–0.38PT layer with its half-wavelength thickness of 2.2 mm (corresponding to the central frequency of 1 MHz), which is commercially available and readily processed.

Further, we studied the influence of the thickness of defect layer to the passband. Fig. 3 shows the peak position and bandwidth of the passband depending on the thickness of the defect layer, whose thickness is symmetrically changed from the half wavelength. The passband shifts towards high frequency (lager than 1 MHz) when the thickness of inserted PMN–PT layer decreases from its half wavelength, and towards low frequency when the thickness is larger than its half wavelength. The transmission efficiency of passband reaches 100% in all studied thickness. These simulated results indicate that the change of the defect thickness can be used to adjust the frequency position of the created passband while keeping the high transmission efficiency.

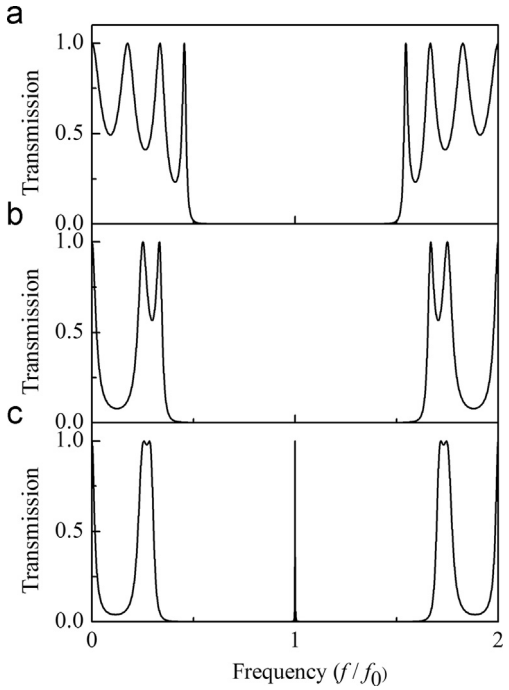

Fig. 2. The transmission spectrum of the 1D phononic crystal containing alternating Al (layer A) and epoxy (layer B) layers. (a) Phononic crystal without defect PMN–0.38PT layer; (b) and (c) phononic crystal containing PMN–0.38PT insertion layer with thickness of $d_C=c_C/4f_0$ and $d_C=c_C/2f_0$, respectively.

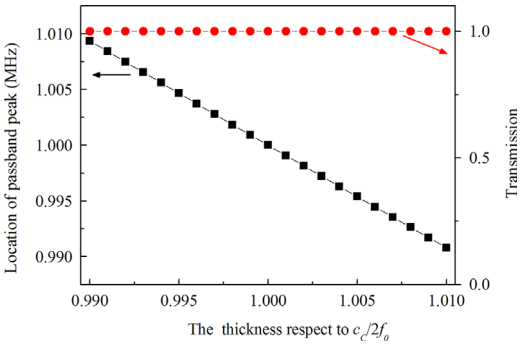

Fig. 3. The effects of the thickness of the PMN–038PT defect layer on the frequency location and transmission characteristics of the passband.

3.2. Effect of strain on passband

The inserted 0.2 mol% Fe-doped PMN–0.38PT defect layer is capable of generating large strain because of its domain switching mechanism [27]. By applying different external voltages onto two compliant electrodes, the piezoelectric layer can be squeezed and stretched in its thickness direction. In Fig. 4, we studied the dependence of passband on the strain of PMN–0.38PT single crystal, which has the original thickness at its half wavelength. One can see that the passband position is dependent on the strain level of the added PMN–0.38PT defect layer. The passbands demonstrated a large shift with the strain increasing as shown in Fig. 4(a), while it presented a nearly invariant bandwidth of about 1.2 kHz at all strains. In Fig. 4(b), we observe that the passband has a shifted frequency up to about 7.4 kHz with 100% wave transmission for the maximum 0.8% strain of inserted single crystal. Note that the passband can move towards high or low frequency depending on the compression or expansion status of the PMN–PT single crystal as shown in Fig. 4(b). Since the strain of the PMN–PT defect layer is closely associated with the external

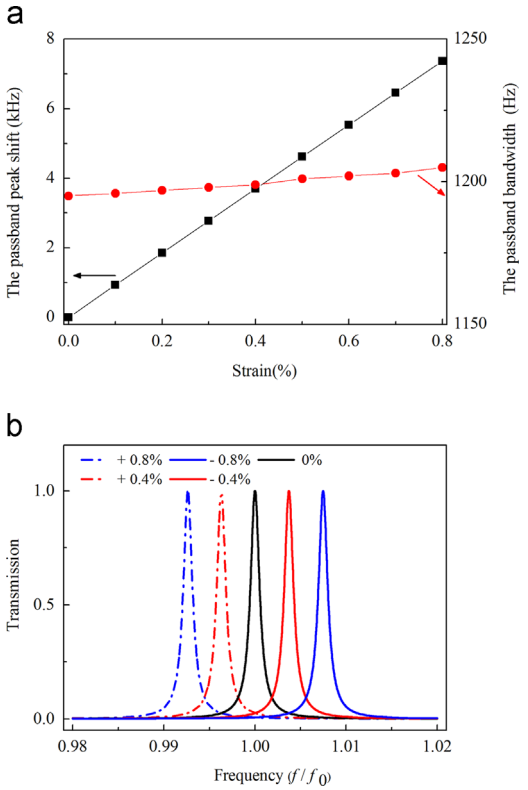

Fig. 4. (a) The dependence of the frequency location and bandwidth of passband on the strain of PMN–0.38PT defect layer; (b) the passband structure at various strain levels of PMN–0.38PT.

voltage [24], the passband can be precisely tuned by applying an electric field at different magnitudes. Thus, the phononic crystal with PMN–0.38PT defect layer may be used as an acoustic switch or frequency screening device, which could be readily controlled by an eternal electric field.

Compared to other functional materials used in tunable phononic crystals, the 0.2 mol% Fe-doped PMN–0.38PT single crystal studied here is capable of producing a giant nonlinear recoverable strain under a relatively low electric field. Feng et al. [24] found that the aged PMN–0.38PT single crystal can reach 0.8% stain at 1.2 kV/mm voltage, which is more than 40 times larger than that of the best PZT ceramics and over 10 times higher than the high-strain PZN-PT single crystal at the same external field [28]. In the aged 0.2 mol% Fe-doped PMN–0.38PT ferroelectric single crystal, the huge recoverable strain under low external field originates from defect-mediated reversible non-180° domain switching by a symmetry-conforming property of point defects. In addition, it was observed that the aged PMN–0.38PT single crystal possesses good temperature stability. Although $BaTiO_3$ single crystal and Mn-doped (Ba, Sr)TiO_3 ceramics are able to generate relatively large recoverable nonlinear strain under low electronic field [28,29], their temperature stability, a very important parameter in the practical acoustic device application, is not satisfactory.

3.3. *Effects of acoustic impedance on passband*

In addition to the frequency position of the passband, its bandwidth is an important parameter determining the axial resolution and spectrum screening of electro-acoustic device. We studied the effects of acoustic impedance of constituent materials in the periodic structure on the passband in Fig. 5. Here, we kept the layers B and C unchanged while replacing layer A with materials at various acoustic impedances, including MgO, Al, Pb,

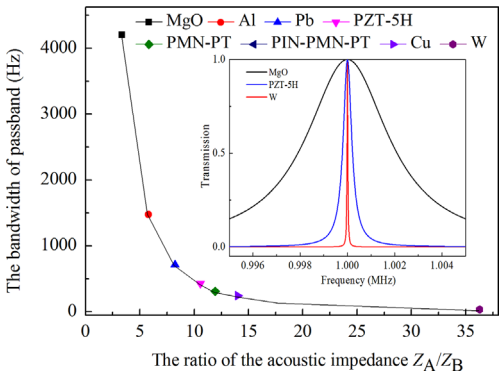

Fig. 5. Influence of the acoustic impedance ratio, Z_A/Z_B, to the passband bandwidth. The inset figure is the representative passband structure of phononic crystal with MgO, PZT-5H and W as layer A.

$[0\,0\,1]_c$ direction PZT-5H ceramic, $[0\,0\,1]_c$ direction 0.2 mol% Fe-doped PMN–0.38PT single crystal, $[0\,\bar{1}\,1]_c$ direction 0.26PIN–0.42PMN–0.32PT single crystal, Cu, and wolfram (W) [30–32]. Fig. 5 shows the bandwidth of the passband as a function of different acoustic impedance ratios of layer A and B, Z_A/Z_B. Obviously, the passband bandwidth decreased with increasing the value Z_A/Z_B. The bandwidth of passband reached up to about 4.2 kHz by inserting MgO as layer A (Z_A/Z_B is 3.4), which is much enlarged compared to phononic crystal containing Al as layer A. For acoustic detection devices, broader bandwidth is helpful for improving depth resolution. The replacement of Al with W produced a narrow passband with 36 Hz bandwidth as shown in the insert of Fig. 5 (Z_A/Z_B is 36.3). This is potentially valuable for precise spectrum screening such as high-sensitivity acoustic switch.

4. Conclusion

In summary, the transmission spectrum of 1D phononic crystal consisting of 0.2 mol% Fe-doped PMN–0.38PT single crystal defect layer has been investigated using the transfer matrix method. By inserting the PMN–0.38PT layer of certain thickness, acoustic passband with 100% transmission efficiency at a specific frequency is induced inside the forbidden gap. Because the thickness of inserted layer predominantly depends on its strain coefficient that can be adjusted by external voltage, the band structure of phononic crystal is tunable by applying an electric field onto PMN–0.38PT single crystal. Moreover, the 0.2 mol% Fe-doped relaxor-based ferroelectric PMN–0.38PT single crystal is capable of generating a large recoverable nonlinear strain based on the point-defect-mediated reversible domain switching mechanism, and thus the passband demonstrates an enlarged frequency shift range (up to 7.4 kHz) under relatively low voltage of 1.2 kV/mm. In addition, the acoustic impedance ratio of layer A and B (Z_A/Z_B) shows significant influence on the bandwidth of the passband, where we observed a narrower passband caused by larger Z_A/Z_B ratio. These calculated results are instructional for developing tunable phononic crystal with an inserted piezoelectric single crystal as the defect layer.

Acknowledgements

This research was supported in part by the National Key Basic Research Program of China (973) under Grant no. 2013CB632900, the Daqing Normal University Youth Foundation no. 12ZR12, the NSFC under Grant nos. 50602009 and 11304061, the China Postdoctoral Science Foundation under Grant no. 2013M531029.

References

[1] M.S. Kushwaha, P. Halevi, L. Dobrzynski, B. Djafari-Rouhani, Phys. Rev. Lett. 71 (1993) 2022.
[2] M. Sigalas, E.N. Economou, Solid State Commun. 86 (1993) 141.
[3] C.Y. Qiu, Z.Y. Liu, Z.M. Jun, J. Shi, Appl. Phys. Lett. 87 (2005) 104101.
[4] A. Cicek, O.A. Kaya, M. Yilmaz, B. Ulug, J. Appl. Phys. 111 (2012) 013522.
[5] M.D. Zhang, W. Zhong, X.D. Zhang, J. Appl. Phys. 111 (2012) 104314.
[6] J. Sánchez-Dehesa, V.M. Garcia-Chocano, D Torrent, F. Cervera, S. Cabrera, J. Acoust. Soc. Am. 129 (2011) 1173.
[7] T.T. Wu, L.C. Wu, Z.G. Huang., J. Appl. Phys. 97 (2005) 094916.
[8] A. Sukhovich, B. Merheb, K. Muralidharan, J.O. Vasseur, Y. Pennec, P.A. Deymier, J.H. Page, Phys. Rev. Lett. 102 (2009) 154301.
[9] J. Bucay, E. Roussel, J.O. Vasseur, P.A. Deymier, A-C. Hladky-Hennion, Y. Pennec, B. Djafari-Rouhani, B. Dubus, Phys. Rev. B: Condens. Matter 79 (2009) 214305.
[10] Y. Pennec, B. Djafari-Rouhani, J.O. Vasseur, A. Khelif, P.A. Deymier, Phys. Rev. E: Stat. Nonlinear Soft Matter Phys. 69 (2004) 046608.
[11] R.H. Olsson , I. El-Kady, Meas. Sci. Technol. 20 (2009) 012002.
[12] C. Goffaux, J.P. Vigneron, Phys. Rev. B: Condens. Matter 64 (2001) 075118.
[13] K. Bertoldi, M.C. Boyce, Phys. Rev. B: Condens. Matter 77 (2008) 052105.
[14] J.Y. Yeh, Physica B 400 (2007) 137.
[15] J.F. Robillard, O.B. Matar, J.O. Vasseur, P.A. Deymier, M. Stippinger, A.C. Hladky-Hennion, B. Djafari-Rouhani, Appl. Phys. Lett. 95 (2009) 124104.
[16] L.Y. Wu, M.L. Wu, L.W. Chen, Smart Mater. Struct. 18 (2009) 015011.
[17] M. Ruzzene, A.M. Baz, Smart Mater. Struct. 9 (2000) 716.
[18] X.Y. Zou, Q. Chen, B. Liang, J.C. Cheng, Smart Mater. Struct. 17 (2008) 015008.
[19] J. Zhao, Y. Pan, Z. Zhong, J. Appl. Phys. 113 (2013) 054903.
[20] S.E. Park, T.R. Shrout, J. Appl. Phys. 82 (1997) 1804.
[21] R. Zhang, B. Jiang, W.H. Jiang, W.W. Cao, Appl. Phys. Lett. 89 (2006) 242908.
[22] E.W. Sun, S.J. Zhang, J. Luo, T.R. Shrout, W.W. Cao, Appl. Phys. Lett. 97 (2010) 032902.
[23] Y.L. Wang, R. Zhang, E.W. Sun, W. Song, W.W. Cao, Chin. Phys. Lett. 30 (2013) 096301.
[24] Z.Y. Feng, O.K. Tan, W.G. Zhu, Y.M. Jia, H.S. Luo, Appl. Phys. Lett. 92 (2008) 142910.
[25] W.W. Cao, W.K. Qi, J. Appl. Phys. 78 (1995) 4627.
[26] Z.L Hou, B.M. Assouar, J. Phys. D: Appl. Phys 41 (2008) 095103.
[27] W.W. Cao, Nat. Mater. 4 (2005) 727.
[28] X.B. Ren, Nat. Mater. 3 (2004) 91.
[29] L.X. Zhang, W. Chen, X. Ren, Appl. Phys. Lett. 85 (2004) 5658.
[30] S.J. Zhu, B. Jiang, W.W. Cao, Proc. SPIE 3341 (1998) 154.
[31] H. Cao, H.S. Luo, Ferroelectrics 274 (2002) 309.
[32] E.W. Sun, W.W. Cao, W.H. Jiang, P. Han., Appl. Phys. Lett. 99 (2011) 032901.